Conf-941006--4
EGG 11265-4012
UC-706

An Image Cancellation Approach to Depth-from-Focus

Shin-yee Lu

Lawrence Livermore National Lab
P. O. Box 80 , L-156
Livermore, CA 94550

Mike Graser

EG&G Energy Measurements, Inc
5667 Gilbraltar Dr.
Pleasanton, CA 94588

ABSTRACT

Depth calculation of an object allows computer reconstruction of the surface of the object in three dimensions. Such information provides human operators 3D measurements for visualization, diagnostic and manipulation. It can also provide the necessary coordinates for semi or fully automated operations. This paper describes a microscopic imaging system with computer vision algorithms that can obtain the depth information by making use of the shallow depth of field of microscopic lenses.

Background

There are many ways of obtaining range (or depth) information. These methods can roughly be classified into two categories: passive and active.[1,2] Active range methods usually require an active source such as a laser and operate in a scanning motion. The typical passive range imaging method uses the principle of stereoscope. Two CCD cameras are mounted in close baseline. The two images obtained from the cameras are registered to generate the image disparities, and range information is calculated by triangulation.

At high magnification (sub-micron resolution), confocal imaging systems use the shallow depth of field of a microscopic lens and scanning laser (or visible light) and detector in coherent motion to generate sharp three dimensional images.[3] In recent years, confocal microscopy has become a powerful tool for biomedical research, as well as semiconductor metrology and inspection.[4] Confocal systems require accurate scanning of mirrors and synchronization of detectors, and complex lens and light beam assembly. It does not lend itself for applications that require miniaturization of the imaging system.

The depth-from-focus approach uses image processing techniques to deduce object depth information from blurring. The advantage is, it does not require stereo imaging heads, nor does it require scanning motion. A number of methods have been developed to solve the depth-from-focus problem, including theoretical derivations of 3D image formation and 3D OTF (optical transfer function)[5], deblurring of individual image sections using serial sectioning[6], range calculation from a single image based on blurring[7], and range calculation from serial sections[8,9]. The 3D OTF shows a missing frequency response which can cause numerical problems. Depth detection based on image blurring is usually very sparse.

In this paper, we will describe the microscopic imaging hardware that is used to obtain optical sections. Optical sections are a series of images obtained from focusing on an object at different depths. We will present an iterative image cancellation algorithm to enhance object surface features at each focal plane. Based on the sharpness of these features, one can determine the focal plane they laid in. The image processing results are illustrated.

Work supported by the U.S. Department of Energy Nevada Operations Office, under Contract No. DE-AC08-93NV11265.

DISCLAIMER

DISCLAIMER

Microscopic Imaging System

Figure 1 shows a block diagram of the imaging system. It uses a 10x microscope objective with a CCD camera chip at the image plane. Illumination is coaxial through-the-lens which is suitable for reflective objects.

A precision motorized stage was used to change the microscope focal position in precise equal steps. The frame grabber captured the stepped image which correspond to the image sections used in the analysis.

An Iterative Image Cancellation Algorithm

We propose a special filter that operates on the difference of an image section and its neighboring section to reduce the blurring contributed from all the other sections. This generates an estimated object surface, which is then used in an iterative procedure to improve the estimation.

In [3], a three-dimensional object is modeled as a stack of object slices located at small intervals along the z-axis,

$$f(x,y,z) = \sum_{i=1}^{n} f(x,y,\Delta z_i). \tag{1}$$

Let f_i be the *ith* slice $f(x,y,\Delta z_i)$. Let p^-_k be the optical point spread function (psf) focused behind the image plane at k slices away. Likewise, p^+_k represents the psf focused in front of the image plane. Assume that p^-_i and p^+_i are approximately the same. Then the 3D image formation of optical sectioning defines the two-dimensional image, focused on slice j to be,

$$I_j = (x,y,z_j) = \sum_{i=1}^{j-1} p_{j-i} * f_i + p_0 * f_j + \sum_{i=j+1}^{n} p_{i-j} * f_i . \tag{2}$$

The iterative procedure first assumes an approximation of the i *th* slice:

$$\kappa_0 * \tilde{f}_j \leftarrow p_1 * I_{j-1} + p_1 * I_{j+1} - (p_0 * I_j + p_2 * I_j). \tag{3}$$

where,

$$\kappa_0 = p_0 + p_2 - 2 p_1 * p_1 . \tag{4}$$

The right-hand side of Eq. (3) can be expanded by substituting each term with Eq (2):

$$\sum_{i=1}^{j-2} (p_0 * p_{j-i} + p_2 * p_{j-i} - p_1 * p_{j-i-1} - p_1 * p_{j-i+1}) * f_i + (p_0 + p_2 - 2 p_1 * p_1) * f_j + \tag{5}$$

$$\sum_{i=j+2}^{n} (p_0 * p_{i-j} + p_2 * p_{i-j} - p_1 * p_{i-j-1} - p_1 * p_{i-j+1}) * f_i .$$

Notice that in Eq. (4) the blurred images from the slices immediately above and below slice j are eliminated. The error induced by the approximation are the first and third terms of Eq. (4), which are the blurred images from slice 1 to $j-2$ from from $j+2$ to n, and an inverse filter κ_0: Let the error caused by the estimation be defined:

$$\Delta f_j = f_j - \tilde{f}_j . \tag{6}$$

then

$$\kappa * \Delta f_j = -\sum_{i=1}^{j-2} \kappa_{j-i} * f_i - \sum_{i=j+2}^{n} \kappa_{i-j} * f_i , \tag{7}$$

where,

$$\kappa_{j-i} = p_0 * p_{j-i} + p_2 * p_{j-i} - p_1 * p_{j-i-1} - p_1 * p_{j-i+1} ,$$

and,

$$\kappa_{i-j} = p_0 * p_{i-j} + p_2 * p_{i-j} - p_1 * p_{i-j-1} - p_1 * p_{i-j+1}.$$

We propose an iterative algorithm that calculates estimated errors and uses the calculated errors to correct the original estimates.

Step 1. Estimate object slices $\tilde{f}_j$

Calculate $\tilde{f}_j$, for $j=1,...,n$,

$$\kappa_0 * \tilde{f}_j \leftarrow p_1 * I_{j-1} + p_1 * I_{j+1} - (p_0 * I_j + p_2 * I_j). \tag{8}$$

Step 2. Generate estimated images

Compute estimated images $\tilde{I}_j$ for $j=1,...,n$ using the estimated object slices,

$$\tilde{I}_j = \sum_{i=1}^{j-1} p_{j-i} * \tilde{f}_i + p_0 * f_j + \sum_{i=j+1}^{n} p_{i-j} * \tilde{f}_i. \tag{9}$$

Step 3. Calculate image error

The difference between an original image I_j and its estimation, $\tilde{I}_j$ is calculated for all $j=1,...n$,

$$\Delta I = I_j - \tilde{I}_j \tag{10}$$

$$= \sum_{i=1}^{j-i} p_{j-i} * \Delta f_j + p_0 * \Delta f_j + \sum_{i=j+1}^{n} p_{i-j} * \Delta f_i.$$

where, Δf_j is defined to be the true object error, and

$$\Delta f_j = f_j - \tilde{f}_j. \tag{11}$$

Step 4. Estimate object error

Calculate $\Delta \tilde{f}_j$, for $j=1,...,n$,

$$k_0 * \Delta \tilde{f}_j \leftarrow p_1 * \Delta I_{j-1} + p_1 * \Delta I_{j+1} - (p_0 * \Delta I_j + p_2 * \Delta I_j). \tag{12}$$

Step 5. Correct object estimates

The estimated object error for slice j is added to the estimated slice j to obtain a new estimate,

$$\tilde{f}^{k+1}{}_j \leftarrow \tilde{f}^k{}_j + \Delta^k \tilde{f}_j. \tag{13}$$

Step 6. Repeat Step 2. to Step 5.

In gereral, the relation between an estimated object error $\Delta \tilde{f}_j$ and the true object error Δf_j at k iteration can be derived,

$$\Delta^k f_j = \Delta^{k-1} f_j - \Delta^{k-i} \tilde{f}_j, \tag{14}$$

where,

$$\kappa_0 * \Delta^k f_j = \sum_{i=1}^{j-2} \kappa_{j-i} * \Delta^{k-1} f_i + \sum_{i=j+2}^{n} \kappa_{i-j} * \Delta^{k-1} f_i, \tag{15}$$

for $k > 1$, and

$$\kappa_0 * \Delta f_j = \sum_{i=1}^{j-2} \kappa_{j-i} * f_i + \sum_{i=j+2}^{n} \kappa_{i-j} * f_i, \tag{16}$$

for k=1; and,

$$\kappa_0 * \Delta^k \tilde{f}_j = \sum_{i=1}^{j-2} \kappa_{j-i} * \Delta^{k-1} \tilde{f}_i + \sum_{i=j+2}^{n} \kappa_{i-j} * \Delta^{k-1} \tilde{f}_i, \tag{17}$$

for $k > 1$, and

$$\kappa_0 * \Delta \tilde{f}_j = \sum_{i=1}^{j-2} \kappa_{j-i} * \tilde{f}_i + \sum_{i=j+2}^{n} \kappa_{i-j} * \tilde{f}_i, \tag{18}$$

for k=1.

Image Processing Results

We took twelve optical sections at 10 micron intervals of a micro-fabricated 3D structure on a silicon substrate. The structure is a 200 micron square frame on a handle pointing upward. Figure 2 (a) to (f) show 6 optical sections, at every other slice out of the original 12 slices. All 12 slices are used in the iterative image cancellation process. Figure 3 (a) to (f) are the corresponding edge enhanced images using the image cancellation method. The edges that are on the specific focal planes are enhanced, and the blurred edges that do not lie in the same focal plane are removed.

The enhanced edges on a focal plane are extracted and labeled by the depth of the focal plane that forms a "range data set", where each pixel is represented by the distance to a reference plane. The depth of the 3D structure in the range image shown in Figure 4 is color coded: lighter color indicates features closer to the viewer, and the darker color indicates features further away from the viewer.

From the range data, we can generate a graphical representation of the 3D surface of the structure. This is shown in Figure 5.

Concluding Remarks

In this paper, we presented a simple imaging system and computer vision algorithm to enhance the object features at each focal plane from a series of optical sections. The computation involves 2-dimensional small kernal convolusions only. The resolutions of optical sections used in our examples are very different in the imaging plane (approx. 0.8 microns per pixel) and along the optical axis (10 microns per slice). The image cancellation approach is not very sensitive to this difference.

Acknowledgment

This work was performed under the auspices of the U.S. Department of Energy by Lawrence Livermore National Laboratory under contract W-7405-Eng-48.

References

[1] D. Nitzan, "Three-Dimensional Vision Structure for Robot Applications," *IEEE Trans. on Pattern Analysis and Machine Intelligence*, Vol. 10, No. 3, May 1988.

[2] Eric P. Krotkov, *Active Computer Vision by Cooperative Focus and Stereo*, Springer-Verlag, 1989.

[3] K. R. Castleman, *Digital Image Processing*.

[4] T. Wilson, *Confocal Microscopy*, Academic Press, 1990.

[5] N. Streibl, "Depth Transfer by an Imaging System," *Optic Acta, 1984, Vol. 31, No. 11, pp. 1233-1241.*

[6] F. Macias-Garza, et. al., "Digital Reconstruction of Three-Dimensional Serially Sectioned Optical Images," *IEEE Transactions on Acoustics, Speech, and Signal Processing*, Vol. 36, No. 7, July 1988.

[7] J. Ens and P. Lawrence, "An Investigation of Methods for Determining Depth from Focus," *IEEE Transactions on Pattern Analysis and Machine Intelligence*, Vol. 15, No. 2, Feb. 1993.

[8] X. Binefa, J. Vitria, and J. J. Villanueva, "Three Dimensional Inspection of Integrated Circuits: a Depth From Focus Approach," *SPIE Proceedings on Machine Vision Application in Character Recognition and Industrial Inspection,* pp. 372-378, Vol. 1991, 1992.

[9] M. Subbarao, T. Choi, "Accurate Recovery of Three-Dimensional Shape from Image Focus," submitted to the IEEE Transaction on Pattern Analysis and Machine Intelligence, 1993.

[10] B. Giord, "Multidimensional range mapping with Pattern Projection and Cross Section," Patent No. 5003166, Issue Date: 1991 03 26.

[11] E. H. Adelson, "Depth-of-Focus imaging process method," U.S. patent no. 4661986, Issue Date: 1987 04 28.

[12] S. Howard, "Pattern Optimization when Measuring Depth to a Surface Using Lens Focusing," U.S. Patent No. 4657393, Issue Date: 1987 04 14.

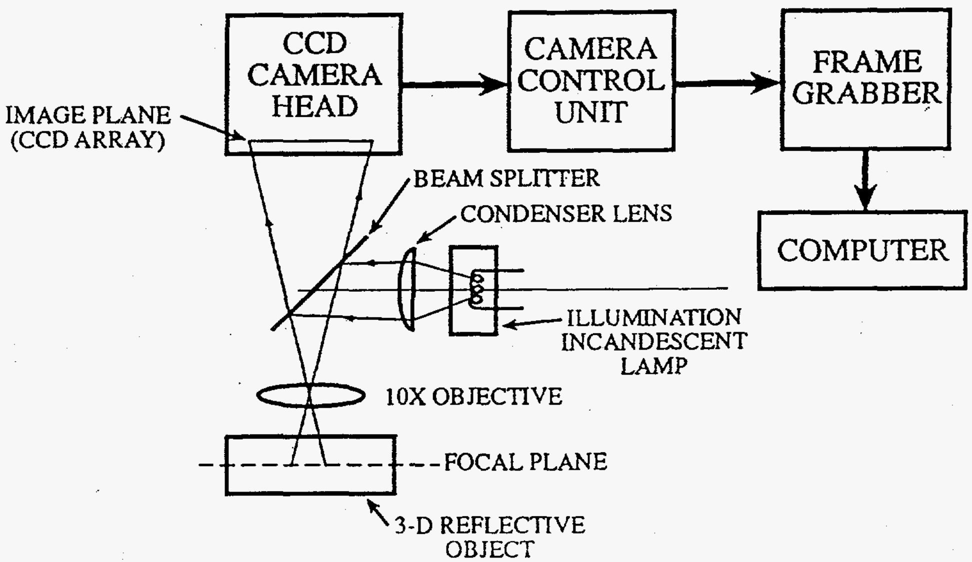

Figure 1. Optical Block Diagram

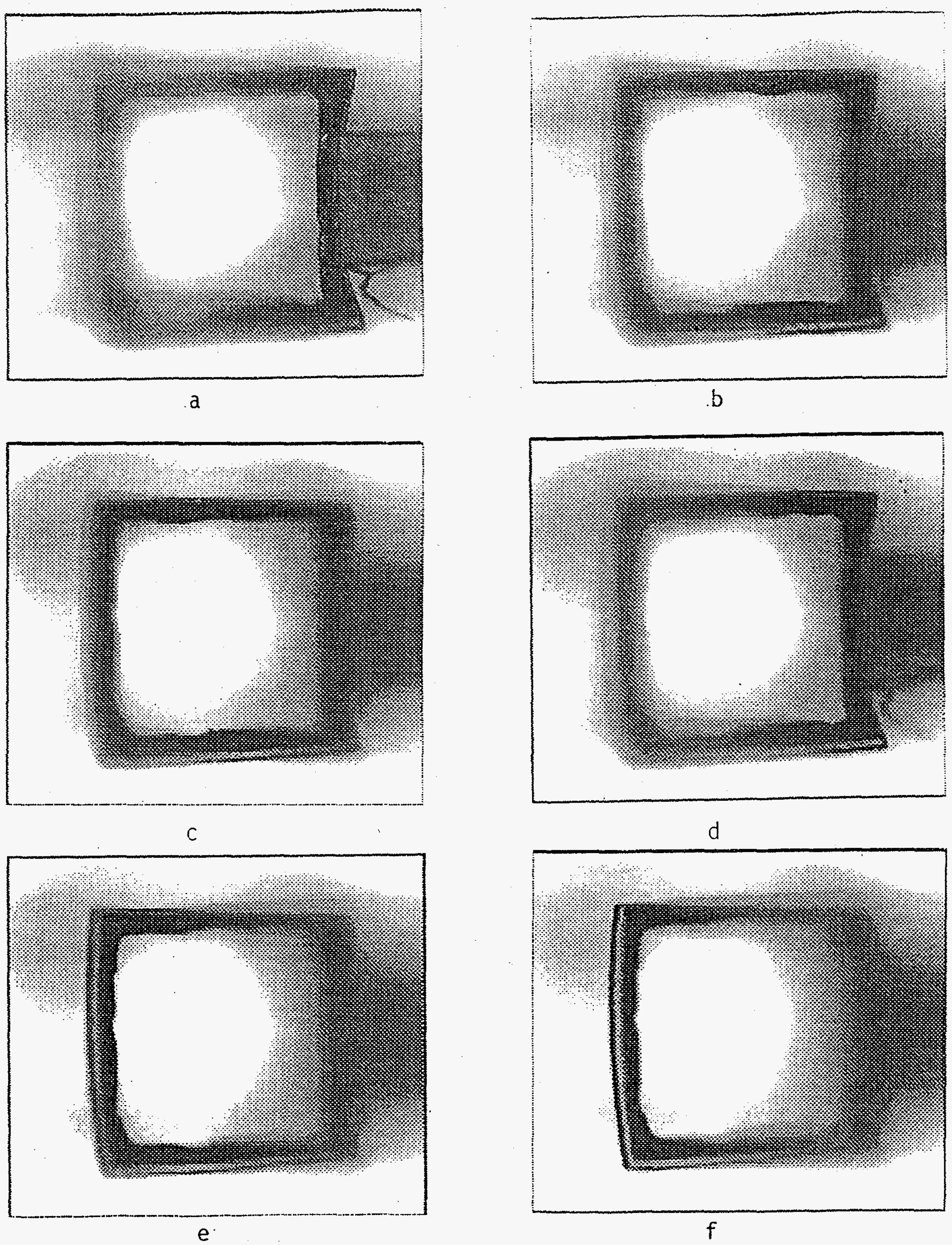

Figure 2. Optical sections of a micro-fabricated structure that is a square frame approximated 200 microns each side on a handle pointing upward. (a) focused at the bottom of the square frame, (b) to (f) focused at 20, 40, 60, 80 and 100 microns above the bottom, respectively.

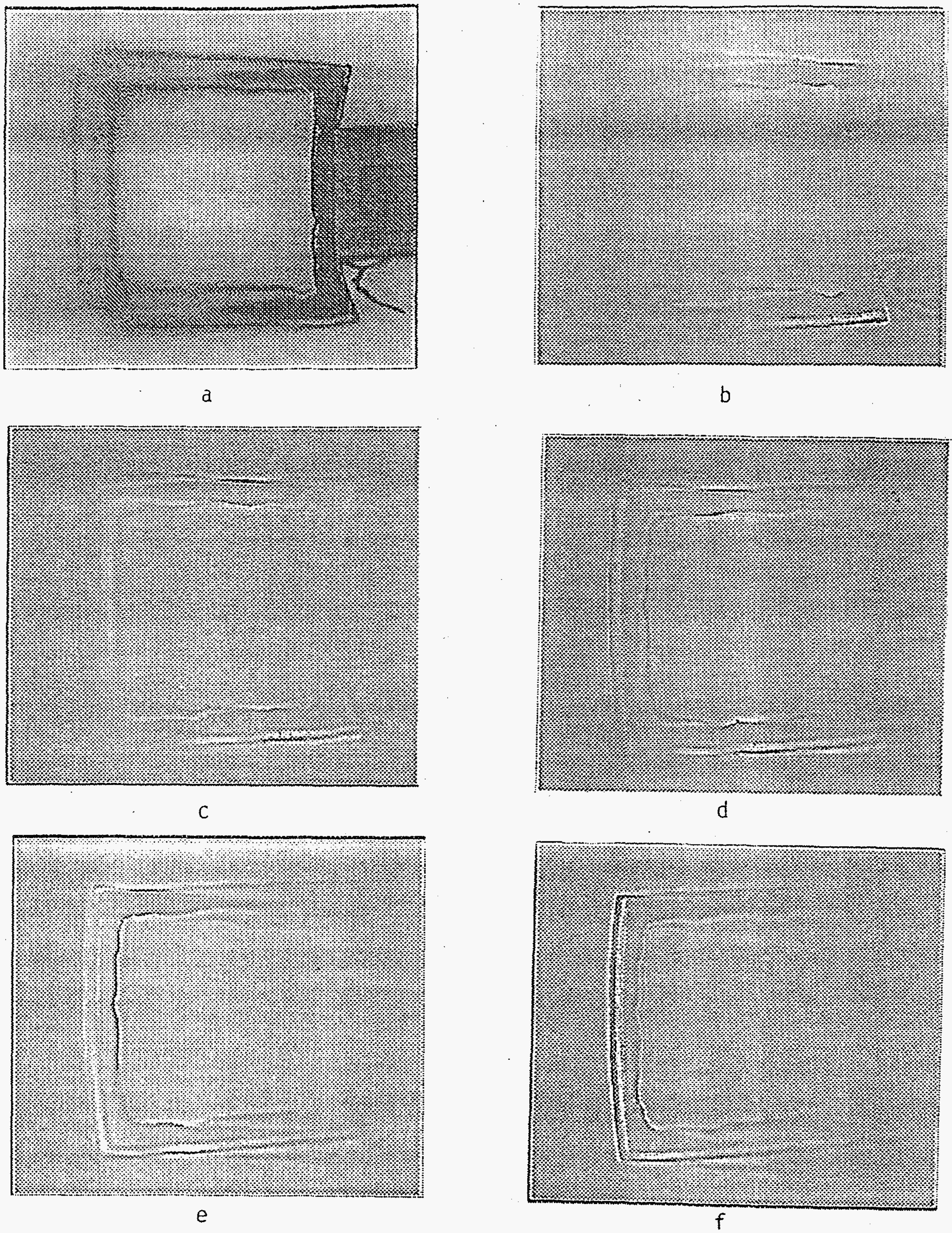

Figure 3. Edge enhanced images of the optical sections using the image cancellation algorithm.

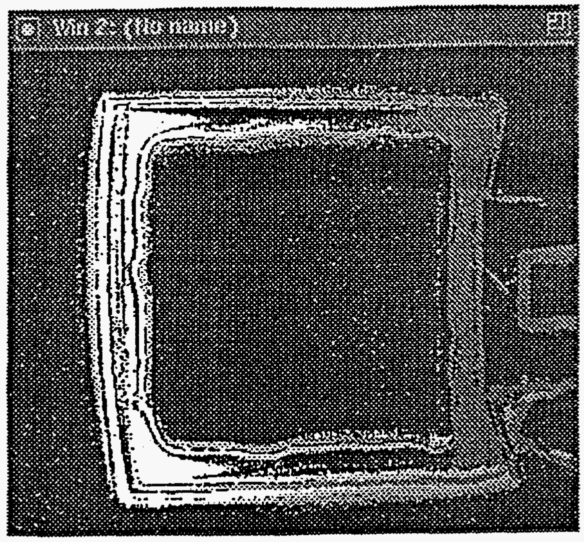

Figure 4. Range image of the micro-fabricated structure, lighter color indicates shallow structure. Darker color indicates deeper structure.

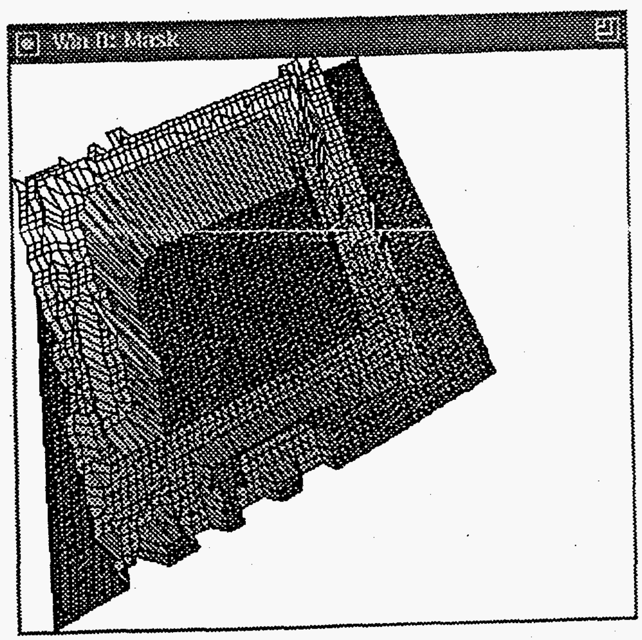

Figure 5. 3D surface reconstruction of the same structure.